10th International Conference on Fracture Mechanics of Concrete and Concrete Structures
FraMCoS-X
G. Pijaudier-Cabot, P. Grassl and C. La Borderie (Eds)
https://doi.org/10.21012/FC10.234090

COMPARISON BETWEEN THE CRACKING PROCESS OF REINFORCED CONCRETE AND FIBRES REINFORCED CONCRETE RAILWAY TRACKS BY USING NON-LINEAR FINITE ELEMENTS ANALYSIS

JEAN-LOUIS TAILHAN, PIERRE ROSSI AND THIERRY SEDRAN

Institut Français des Sciences et Technologies des Transports, de l'Aménagement et des Réseaux (IFSTTAR), Université Paris-Est, France
e-mail: jean-louis.tailhan@ifsttar.fr, Pierre.rossi@ifsttar.fr, thierry.sedran@ifsttar.fr

Key words: Probabilistic Explicit Cracking Model, Fiber Reinforced Concrete, Reinforced Concrete, Railway tracks

Abstract: The present work concerns the use of probabilistic explicit cracking models to analyze the cracking process of two types of Railway Tracks: the first one in reinforced concrete and the second one in fibres reinforced concrete

1 INTRODUCTION

Steel fiber reinforced concrete (SFRC) is increasingly used in structural applications. One of the principal reasons of its gain in popularity is due to the existence of national and international recommendations for the design of structures using this type of material. These recommendations are efficient for designing simply supported structural elements subjected to bending. However, they do not possess a sufficient physical base to propose relevant solutions for more complex structures such as these statically indeterminate. Hence, it is claimed that the most efficient approach for designing such structures with respect to both safety and sustainable development is to use non-linear finite element analysis.

IFSTTAR has been developing, since 1985, a probabilistic explicit cracking model to simulate the cracking process of concrete. Then, this model was extended to analyze reinforced concrete and fibre reinforced concrete structures. All these numerical models have been, today, fully and deeply validated [1-9].

The present work concerns the use of these numerical models to analyze the cracking process of two types of Railway Tracks: the first one in reinforced concrete and the second one in fibres reinforced concrete. In fact, this comparative analysis is performed on a large mockup designed to represent, reasonably well, the reality.

2 DESCRIPTION OF THE IFSTTAR RAILWAY TRACK MOCKUP

The mean objective behind the design of the IFSTTAR Railway Track Mockup is to get a representative structural situation and to perform mechanical tests on it. Figure 1 presents the selected mockup geometry.
In this figure, BC5 represents the track slab and BC3 the foundation slab. A Sylomer layer is used to take into account the mechanical reaction of the ground.

Figure 2 presents the mechanical loading applied to the Railway Track Mockup.

It is important to note that, added to this external mechanical loading, the dead load generated by the rails, the pads and the plates as well as thermal loadings (positive and negative gradients) are considered in all numerical simulations of this study.

Figures 3 and 4 present respectively the

positive and negative gradients taken into account in the numerical simulations.

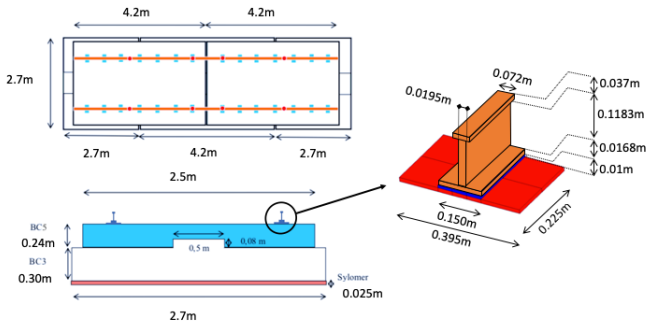

Figure 1. Geometry and dimensions of the IFSTTAR Railway Track Mockup

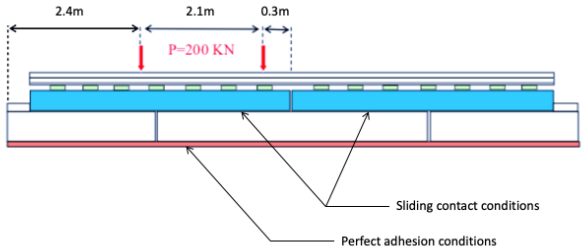

Figure 2. Loading conditions on the mockup.

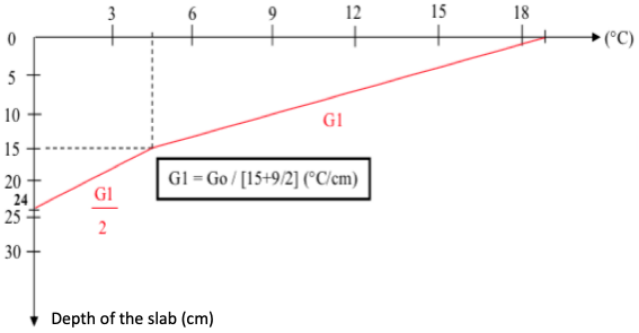

Fig. 3. Positive thermal gradient used in the numerical simulations.

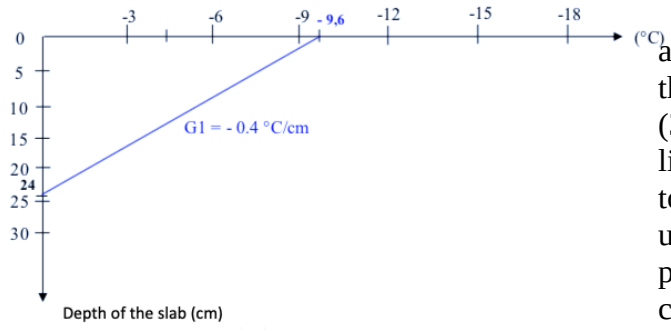

Fig. 4. Negative thermal gradient used in the numerical simulations

3 FINITE ELEMENTS MESHES, MECHANICAL ASSUMPTIONS, BOUNDARY CONDITIONS AND MATERIALS MECHANICALS CHARACTERISTIC UNDERLYING THE NUMERICAL SIMULATIONS

The objective of the work is to perform a comparison between the cracking process of, both, Reinforced Concrete Railway Track (RCRT) and Fibres Reinforced Concrete Railway Track (FRCRT) by using non-linear finite elements analysis. Figures 5 and 6 present the finite elements meshes related respectively to RCRT and FRCRT solutions.

Concerning the RCRT, the total section of rebars at the top and at the bottom of the track slab are, respectively, $\boldsymbol{1.53\ 10^{-3}\ m^2}$ and $\boldsymbol{3.38\ 10^{-3}\ m^2}$.

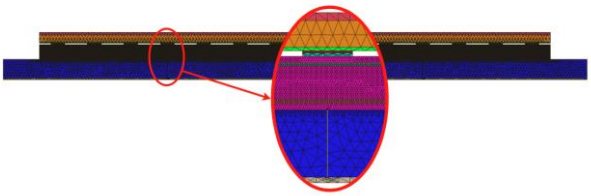

Figure 5. 2D finite element mesh related to the numerical simulations of the RCRT.

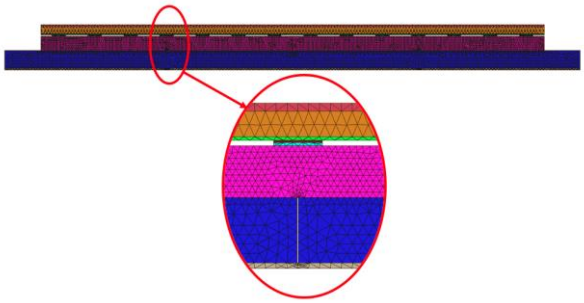

Figure 6. 2D finite element mesh related to the numerical simulations of the FRCRT

As observed on these figures, the meshes are two-dimensional (2D). Indeed, although the mechanical problem is a three-dimensional (3D) one, it is unreasonable to perform non-linear 3D simulations which should consume too much computational time with the models used. The numerical simulations are then performed under 2D and plane stress conditions, since these specific models also take into account volume effects (see chapter 4) and the width (i.e. the length measured in

the direction perpendicular to the plane of the figure) of the mockup has to be considered.

For the reason related to volume effects (see chapter 4), considering the total width of the mockup will cause the models to produce a poor description of the cracking processes. But nevertheless, a more detailed description of the cracking processes can be achieved by choosing to perform simulations with a smaller value of this width; since, of course, the simulation also gives acceptable information about the longitudinal distribution of the elastic tensile stresses at the bottom of the track slab (where cracks will be created) compared with 3D simulation.

The width of the cast iron plates under the rail, and equal to ***0.395 m*** (see Figure 1), seems to be the smaller one it is reasonable to consider in the present 2D numerical analysis. This choice leads to underestimate the real stresses diffusion under the rails and, so, to underestimate the global stiffness of the mechanical system (all the mockup). To solve this problem, one possible solution is to increase the Young modulus of the materials constituting the mechanical system, especially for the track and foundation slabs and the sylomer (where the stresses are diffused). To achieve this objective, the following steps of numerical simulations have been performed:

- First step: 3D elastic simulation of the full mockup with the real stiffness of the materials. Figure 7 presents the 3D mesh used for this numerical analysis.
- Second step: 2D elastic simulation (plane stresses conditions) with the full width of the track slab mockup and with the real stiffnesses of the materials.
- Third step: 2D elastic simulations with smaller widthes of the mockup and different values of stiffness related to the different materials.

Remark: In all these numerical simulations (3D and 2D), the rebars are not taken into account.

This search of the best of materials stiffness related to the 2D simulation on the reduced mockup width leads to the values summarized in Table 1.

Table 2 presents the values of the others materials properties used in the framework of these elastic numerical simulations. They are independent of the type of linear numerical simulation performed.

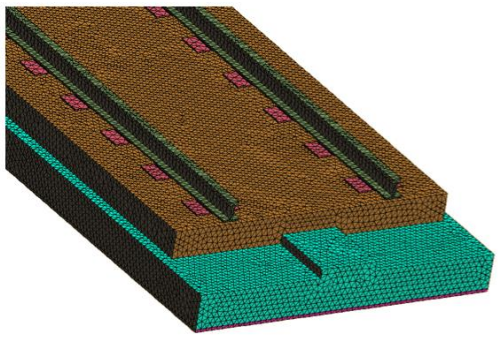

Figure 7. 3D mesh of the mockup

Table 1. Values of the materials Young modulus used in the elastic numerical simulations.

	Young modulus (MPa)		
	3D Simulation	2D Simulation full wide	2D Simulation reduced wide
Rails	210000	210000	210000
Soles	7.702	7.702	7.702
Iron Saddles	17200	17200	17200
Track Slab	35000	35000	43750
Foundation Slab	24000	24000	32500
Sylomer	1.2	1.2	1.625

Table 2. Values of the others materials properties used in the elastic numerical simulations.

	Poisson coefficient	Density
Rails	0.3	7.8
soles	0.4	1.2
Iron Saddles	0.3	7.8
Track Slab	0.25	2.5
Foundation Slab	0.25	-
Sylomer	0.32	-

Figure 8 presents the longitudinal tensile stresses distribution at the bottom of the track slab given by the three types of elastic analysis.

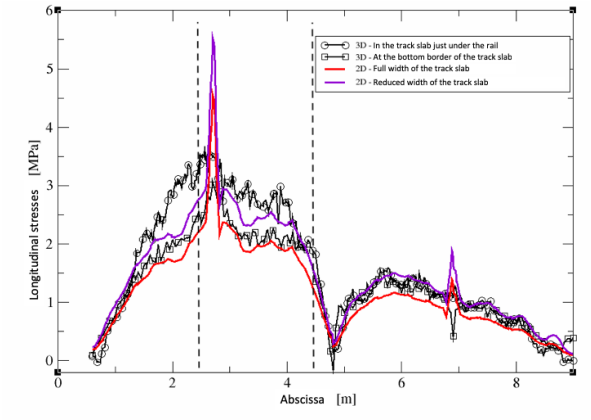

Figure 8. Longitudinal tensile stresses distribution at the bottom of the track slab given by the three types of elastic analysis.

In the light of this linear elastic study, it can be considered as acceptable to perform the non-linear 2D finite elements simulations on the proposed reduced wide of the mockup.

4 NUMERICAL MODELS USED IN THE NON-LINEAR FINITE ELEMENTS SIMULATIONS

4.1 Probabilistic Explicit Cracking Model of Concrete

The model was first developed at IFSTTAR (formerly LCPC) by Rossi [10-12] and recently improved by Tailhan et al. [13]. It describes the behaviour of concrete via its two major characteristics: heterogeneity, and sensitivity to scale effects [14]. The physical basis of the model (presented in detail in [10-12]) can be summarized as follow:

- The heterogeneity of concrete is due to its composition. The local mechanical characteristics (tensile strength f_t, shear strength τ_c) are randomly distributed.
- The scale effects are a consequence of the heterogeneity of the material. The mechanical response directly depends on the volume of material that is stressed.
- The cracking process is controlled by defects in the cement paste, by the heterogeneity of the material, and by the development of tensile stress gradients.

The following points specify how the numerical model accounts for these physical evidences:

- The model is developed in the framework of the finite element method, each element representing a given volume of heterogeneous material.
- The tensile strength is distributed randomly over all elements of the mesh using a Weibull distribution function whose characteristics depend on the ratio: *volume of the finite element/volume of the largest aggregate*, and the compressive strength (as a good indicator of the quality of the cement paste). The volume of the finite element depends on the mesh, while the volume of the largest aggregate is a property of the concrete [10-12].
  Remark: a Weibull distribution function is the best to take into account the rupture in tension of a brittle and heterogeneous material as concrete.
- The shear strength is also distributed randomly over all elements using a distribution function: (1) its mean value is independent of the mesh size and is assumed equal to the half of the average compressive strength of the concrete and (2) its deviation depends on the element size, and is the same (for elements of same size) as that of the tensile strength.

Concerning the cracks representation, two approaches are proposed, depending if 2D or 3D numerical simulations are concerned [13].

In what follows, only aspects related to 2D models are presented.

In 2D simulations, the cracks are explicitly represented by 2D non-linear interface elements (quadratic elements) of zero thickness. These elements connect volume elements representing un-cracked plain concrete. Failure criteria of Rankin in tension and Tresca in shear are used. As far as tensile or shear stresses remain lower than their

critical values, the interface element ensures the continuity of displacements between the nodes of its two neighboring volume elements. The material cell gathering these two volume elements and the interface element remains therefore elastic. Once one of the preceding failure criteria is reached, the interface element opens and an elementary crack is created. The tensile and shear strengths as well as the normal and tangential stiffness values, related to this interface element, become equal to zero [10-12]. In case of crack re-closure, the interface element recovers its normal stiffness and follows a classical Coulomb's law [10-12].

Note that in this modelling approach, the creation and the propagation of a crack is the result of the creation of elementary failure planes that randomly appear and can coalesce to form the macroscopic cracks (Figure 9).

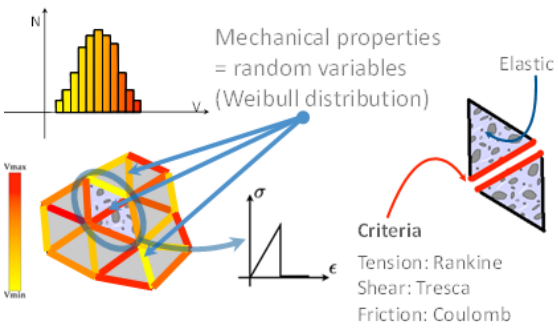

Figure 9. Probabilistic concrete cracking model – explicit approach

4.2 Probabilistic Explicit Cracking Model of Fibres Reinforced Concrete (FRC)

The creation of cracks in the concrete matrix is represented by an elastic perfectly brittle behaviour, whereas the bridging effect of the fibres is described by the following modelling approach.

Normal and tangential stresses in the interface element linearly increase with normal and tangential displacements when a "broken" interface element re-opens to take into account the elastic bridging effect of the fibres inside the crack. Physically speaking, the rigidity of the fibres (inside the cracks) is more important in tension than in shear. Thus, the interface element rigidity is considered different for normal and tangential displacements. In 2D, normal and tangential rigidities of the interface element are K_n' and K_t' respectively. The post-cracking elastic behaviour exists until it reaches a threshold value, ζ_0, related to the normal displacement (Figure 10). The mechanical behaviour of the interface element changes once this threshold value is reached. The normal stress is considered as linearly decreasing with the normal displacement in order to take into account the damage of the bond between the concrete and the fibre, and fibre pullout. The decreasing evolution is obtained by using a damage model.

Finally, the interface element is considered definitively broken when the normal displacement reaches a threshold value, ζ_c (Figure 10). This value corresponds to the state where the effect of fibres is considered negligible. It is determined from a uniaxial tensile test. At this point, its normal and tangential rigidities are set to zero.

The post-cracking energy dissipated by the bridging effect of the fibres is considered randomly distributed over the mesh elements. The random distribution chosen is a log-normal distribution function with a mean value independent of the mesh elements size [15] and a standard deviation, due to the heterogeneity of the material, increasing as the mesh elements size decreases. The choice of a log-normal distribution function is an arbitrary one. It is convenient to avoid having negative values of the post-cracking energy when the element meshes are very small. To model a given structural element, the distribution function is determined in the following manner:

- The mean value is directly obtained experimentally from a certain number of uniaxial tensile tests on notched specimens, more specifically from the load-crack opening experimental curves (it is the best way of determination). If the uniaxial tensile tests have not been performed, that mean value can be determined also by analysing bending test results using an inverse approach.
- The standard deviation, which depends on the mesh elements size, is determined

by an inverse analysis approach that consists of simulating the uniaxial tests with different element mesh sizes. As the mean value of the post-cracking energy is known from the experimental results, several numerical simulations are realized for each mesh size to determine the standard deviation that best fits the experimental results. The inverse analysis approach thus allows finding a relation between the standard deviation and the finite element mesh size. As for the mean value, the standard deviation can be determined by analysing bending test results using an inverse approach.

The threshold parameters ζ_0 and ζ_c are determined by an inverse analysis approach to best fit the simplified triangular stress-displacement curve representing the post-cracking energy (Figure 10) to the experimental tensile softening curve.

Figure 10) presents the numerical mechanical behaviour adopted to represent the experimental post-cracking behaviour. Only the *normal stress-normal displacement* curve is considered in this figure.

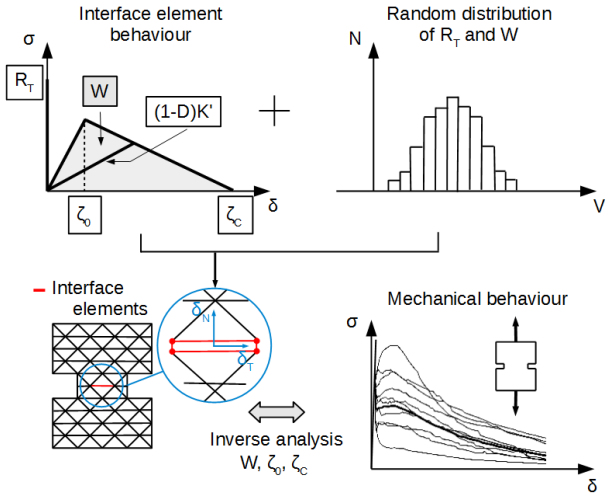

Figure10. Probabilistic FRC model

4.3 Rebars and concrete/steel bond modelling

The rebars are considered, in the 2D modelling approach, as equivalent plates mixing concrete and steel rebars. The reinforcement ratio at the top of the track slab being different of the one located at the bottom, two equivalent plates are considered in the simulations. The heigths of these plates are taken equal to the greater diameter of the local rebars. The Young moduli of the plates are determined by using a classical mixture rule (see relation 1).

$$E = (E_a A_a + E_b A_b)/(A_a + A_b) = (A_b/A_a + A_b)\,[E_b + t_a E_a] \quad (1)$$

Where: E_a and E_b are respectively the steel and the concrete Young moduli; A_a and A_b are respectively the steel and the concrete sections; t_a is a local reinforcement ratio (for the considered plate).

Table 3 presents the values related respectively to the height, the width, the Young modulus and the Poisson coefficient of the equivalent plates in the simulations.

Table 3.Values related respectively to the high, the wide, the Young modulus and the Poisson coefficient of the equivalent plates in the simulations.

	High (m)	Wide (m)	t_a (%)	E (MPa)	ν
Top plate	0.014	0.395	3.81	41646	0.25
Bottom plate	0.016	0.395	8.81	50506	0.25

ν is the Poisson Coefficient

Numerically speaking, the equivalent plates are composed of one layer of volume elements. Here again, the volume elements are all interfaced by interface elements. These interface elements permit the crack crossing through the equivalent plates. They are exactly the same that those used to model concrete cracking and follow the same opening criteria (see chapter 4.1). In this case, the volume of concrete considered for each opening of interface element (see chapter 4.1) is that of the cumulated volume of elements surrounding it (it is, of course, an approximation).

After the opening of interface element, its residual stiffness is calculated considering these two following assumptions:

- The interface element section considered is that of the equivalent plate crossed by the crack.
- A total rupture of adherence along the two volume elements concerned by the interface element is assumed.

5 NON-LINEAR NUMERICAL SIMULATIONS

The parameters values (in relation with the size of finite element meshes, see chapter IV) used in the non-linear simulations are given in Table 4.

Table 4. Parameters values used for cracking of concrete and FRC.

Parameter		Value
RT	Mean value	4.87 [MPa]
	Standard deviation	0.67 [MPa]
W	Mean value	4.26 10^{-3} [MPa.mm]
	Standard deviation	2.6 10^{-3} [MPa.mm]
ζ_0		50 [µm]
ζ_c		4 [mm]

The FRC considered in this study is taken from the literature and used in a previous numerical study [6]. This FRC contains 78 kg/m^3 of steel fibres. These fibres are hooked end ones.

In this paper are presented results related only to positive temperature gradient. Indeed, negative temperature gradient has led to very less and smaller cracks compared with those related to positive temperature gradient.

In Figure 11 are presented cracking patterns of the FRC track slab related to 3 different simulations (with different random distributions).

In Figure 12 is presented a more detailed information of this cracking pattern (one of the three simulations of the FRC track slab is concerned).

In Figure 13 are presented cracking patterns of the reinforced track slab related to 3 different simulations (with different random distributions).

In Figure 14 is presented a more detailed information of this cracking pattern (one of the three simulations of the reinforced track slab is concerned).

Considering Figures 11 to 14, the following comments can be made:

- When the tensile stresses in the track slab are localized (isostatic situation), like at the vertical of the joints of the foundation slab, only one crack appears, and the crack opening is smaller for the reinforced concrete track slab than for the FRC track slab.
- On the contrary, when the tensile stresses in the track slab are diffused (statically indeterminate situation), like between two joints of the foundation slabs, the cracks openings are clearly smaller in the case of FRC track slab.

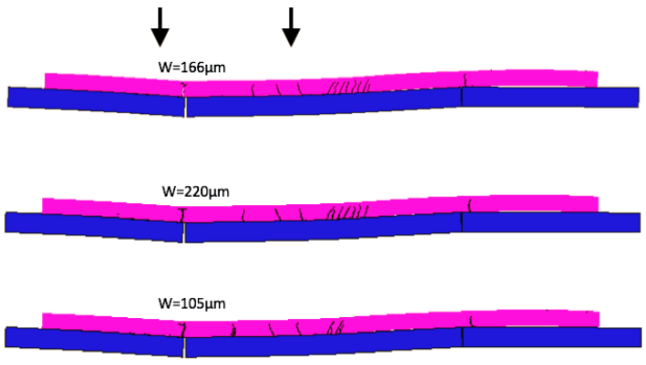

Figure 11. Cracking patterns related to the FRC track slab – 3 simulations – Positive temperature gradient and loading effort of 200 kN – w is the crack opening.

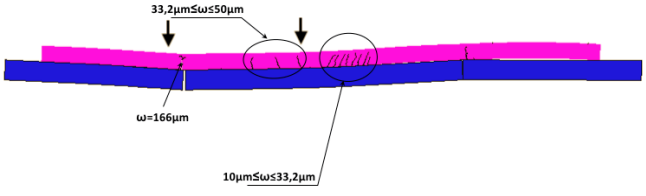

Figure 12. Cracking pattern related to the FRC track slab – Detailed information about one simulation – w is the crack opening.

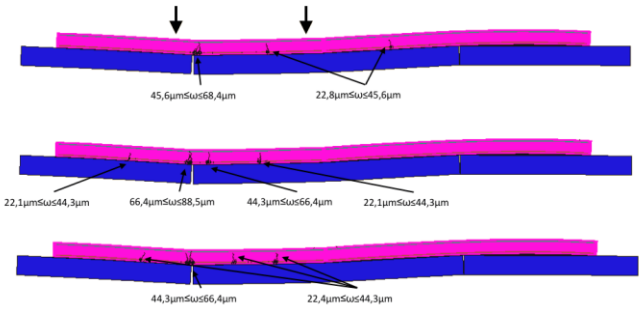

Figure 13. Cracking pattern related to the reinforced track slab – 3 simulations – Positive temperature gradient and loading effort of 200 kN.

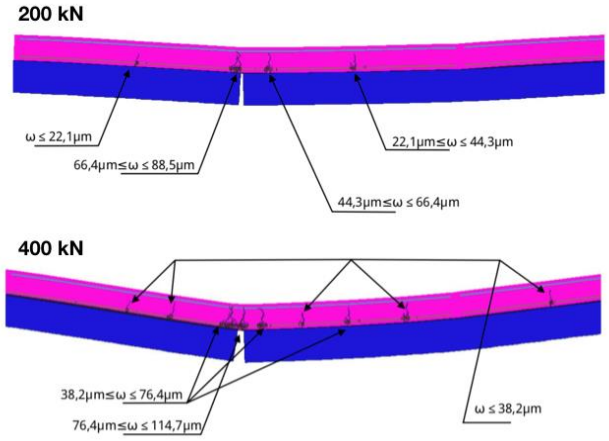

Figure 14. Cracking pattern related to the reinforced track slab – Detailed information about one simulation.

5 CONCLUSIONS AND PERSPECTIVES

This study concerns the use of numerical models to analyze and compare the cracking process of two types of Railway Tracks: one in reinforced concrete and the second one in FRC. The models used are Probabilistic Explicit Cracking ones developed by IFSTTAR and fully validated in the framework of previous works.

The main result obtained can be summarized as following:

- When in a given concrete structure, the tensile stresses are localized, the traditional rebars are more efficient to control cracks than the presence of fibres. For that, it is necessary, of course, to get an easy and optimal placement of the rebars in relation with cracks orientation. That is the case in railway tracks.
- On the contrary, when the tensile stresses are diffused, that is the case in statically indeterminate mechanical situations, the fibres are significantly more efficient than traditional rebars in regards to this cracks control. The parts of the railway track slabs which are located between the zones delimited by the joints in the foundation slab are concerned by this conclusion.

For the practice, it can be argued that, for railway track slabs; the use of 78 kg/m^3 de fibres is mechanically more efficient than the usual ratio of rebars. On the other hand, if this technical solution is adopted, it is preferable to use, in zones of high concentration of tensile stresses, some local rebars (low quantity) to ensure a necessary level of safety to the structure.

In the future, it would be interesting to perform experimental tests on the reinforced concrete and FRC mockups concerned by this study to confirm the present results.

It should be nice also, to use the numerical models presented in this work to propose an optimization of the structural design of the SFR track slab (percentage of fibres, slab thickness…).

REFERENCES

[1] Phan, T. S., Tailhan, J-L and Rossi, P., 2013. 3D numerical modelling of concrete structural element reinforced with ribbed flat steel rebars, *Structural Concrete*, 14.4: 378-388.

[2] Tailhan, J.L., Rossi, P., Daviau-Desnoyers, D., 2015. Numerical modelling of cracking in steel fibre reinforced concrete (SFRC) structures, *Cement and Concrete Composites*, vol. 55, pp. 315-321.

[3] Rossi, P., Daviau-Desnoyers, D., Tailhan, J.L., 2015. Analysis of cracking in steel fibre reinforced concrete (SFRC) structures in bending using probabilistic modelling. *Structural Concrete*, 16(3):381–388.

[4] Rastiello, G., et al., 2015. Macroscopic probabilistic cracking approach for the numerical modelling of fluid leakage in concrete. *Annals of Solid and Structural Mechanics*, 7(1-2):1–16.

[5] Rossi, P., et al., 2016. Numerical models for designing steel fiber reinforced concrete structures: why and which ones? *FRC 2014: ACI-fib International Workshop*, Editors: B. Massicotte, J.-P. Charron, G. Plizzari, B. Mobasher, *FIB Bulletin 79 – ACI SP-310*, 289-300.

[6] Rossi, P., Tailhan, J.L., 2017. Numerical modelling of the cracking behaviour of steel fibre reinforced concrete (SFRC) beam on grade, *Structural Concrete*, 18 (4), pp.571-576.

[7] Rossi, P., Daviau-Desnoyers, D., Tailhan, J.L., 2018. Probabilistic Numerical Model of Ultra-High Performance Fiber Reinforced Concrete (UHPRFC) Cracking Process, *Cement and Concrete Composites*, vol. 90:pp. 119-125.

[8] Nader C., Rossi, P., Tailhan J.L., 2017. Numerical strategy for developing a probabilistic model for elements of reinforced concrete, *Structural Concrete*, 18 (6), pp.883–892.

[9] Nader C., Rossi, P., Tailhan J.L., 2018. Multi-scale Strategy for Modelling Macrocracks Propagation in Reinforced Concrete Structures. *Cement and Concrete Composites*, htts://doi.org/10.1016/j.cemconcomp.2018.04.012.

[10] Rossi P., Richer S., 1987. Numerical modelling of concrete cracking based on a stochastic approach, *Materials and Structures*, vol. 20, pp. 334-337.

[11] Rossi, P., Wu, X., 1992. Probabilistic model for material behaviour analysis and appraisement of concrete structures, *Magazine of concrete research* 44.161: 271-280.

[12] Rossi, P., Ulm, F-J, Hachi, F., 1996. Compressive behaviour of concrete: physical mechanisms and modeling, *Journal of Engineering Mechanics* 122.11: 1038-1043.

[13] Tailhan J.L.; Dal Pont S.; Rossi P., 2010. From local to global probabilistic modelling of concrete cracking, *Ann. Solid. Struct. Mech*., vol. 1, pp. 103-115.

[14] Rossi, P., Wu, X., Le Maou, F., Belloc, A., 1994. Scale effect on concrete in tension, Materials and Structures, vol. 27, pp. 437-444.

[15] Rossi, P., 2012. Experimental Study of Scaling Effect Related to Post-Cracking Behaviours of Metal Fibres Reinforced (MFRC), *European Journal of Environmental and Civil Engineering*, 16(10): 1261-1268.